Hindawi
Advances in Materials Science and Engineering
Volume 2023, Article ID 2141115, 16 pages
https://doi.org/10.1155/2023/2141115

Research Article

Corrosion Resistant Coating from Nano Printed Circuit Board Powder for the Reinforced Concrete Structures

R. Mohana,[1] **D. Selvaganesh**,[1] **A. Anto Issac**,[1] **and M. Vignesh Kumar**[2]

[1]*Department of Civil Engineering, Mepco Schlenk Engineering College, Sivakasi, India*
[2]*Construction Technology and Management, Wollega University, P.O. Box 395, Nekemte, Oromia Region, Ethiopia*

Correspondence should be addressed to M. Vignesh Kumar; vignesh@wollegauniversity.edu.et

Received 12 October 2022; Revised 5 December 2022; Accepted 8 April 2023; Published 20 April 2023

Academic Editor: P. Madindwa Mashinini

Corrosion in steel leads to the deterioration of reinforced concrete structures due to chemical reactions between steel and its surrounding atmosphere. In this paper, a novel anticorrosive powder was derived from the waste Printed Circuit Board (PCB) and manually coated on the steel rebar of the reinforced concrete specimen. The corrosion-resistant efficiency of the developed nano PCB-coating on the steel bars was studied by polarization, electrochemical impedance spectroscopy, and accelerated corrosion technique. Also, the applicability of the nano PCB-coated rebar as reinforcement in the concrete environment was investigated. From the results, it was observed that the nano PCB-coated specimens exhibited 3.5 times reduced rate of corrosion and lost only 46.15% strength and 52.5% diameter under the accelerated rate of 6 V after 48 hours. The presence of nano PCB powder improved the corrosion-resistant behaviour of the steel rebar by 1.65 times of the noncoated specimen. Also, the nano PCB-coating reduced the loss in residual yield strength of the corroded steel rebar by 32% lesser than the noncoated specimens and exhibited similar corrosion-resistant properties as that of the existing zinc coating. In addition to the corrosion resistance, the nano PCB-coated steel rebar exhibited almost similar adhesion with concrete as that of the commercial zinc coating which is 7% lower than uncoated steel rebars. It was inferred from this research work that the proposed anticorrosive coating prepared from the waste nano PCB powder showed better corrosion-resistant behaviour and reduced the overall cost of coating by 42%, which ensures economy and serviceability.

1. Introduction

Corrosion is the most challenging phenomenon faced by the construction industry, which necessitates the maintenance cost of 2.5–5% of gross domestic product cost expensed by each country per annum. In this series, next to Arabian countries, India and China individually spend 4.2 billion US$ annually, which is the second largest expenditure to control corrosion [1]. Due to the continuous permeation of external ions through the voids of the concrete, corrosion in steel cannot be eliminated, but the corrosive mechanism can be controlled and retarded by using galvanizing and anti-corrosive coatings [2]. Al-Negheimish et al. [3], alloyed zinc with aluminium in order to improve the corrosion resistance of hot dip galvanized coated bars in contact with chloride-contaminated concrete. It was found that 10% aluminium and 90% zinc showed higher corrosion resistance performance than 100% Zinc-coated rebar.

Similarly, Sharma et al. [4], carried out research work to reduce the effects of corrosion by adding nano-clay and tung oil microcapsules. The nano-clay-modified epoxy coatings showed a significant delay in the breakdown of the passive layer on the rebar. On the other side, tung oil microcapsule in urea formaldehyde shells were prepared by in-situ polymerization to improve the self-healing ability and adhesion strength of capsule-embedded coatings and act as self-healing agents. Overall, corrosion drops by the addition of nano-clay are at least by a factor of 3 and due to tung oil microcapsule is at least by an order of magnitude. Shaikh and Sheetalsahare [5] carried out the research work on the impressed current technique to accelerate the rate of corrosion of steel reinforcing bars in concrete for three different

voltages. They observed that the level of voltage had no effect on the final crack pattern. The concrete crack pattern and the mass loss due to accelerated corrosion up to the development of the first visible crack on the concrete specimen were evaluated. Feng and Cheng [6], carried out the research work to find out corrosion resistance in magnesium alloys investigated by the EIS technique in ceria-based coatings and pigments. It was concluded that the bare specimen had lower impedance than the coated specimen. They also indicated that the proper acid treatment on the surface resulted in better corrosion resistance.

Dixit and Gupta [7], studied the corrosion assessment in rebars by impressed current technique. While observing the time required for the initiation of the first noticeable cracks, it was observed that the variation of the degree of corrosion is proportional to the applied current. Jagtap et al. [8], studied the effect of zinc oxide in combating corrosion in zinc-rich primer and suggested that the combined use of zinc and zinc oxide resulted in better corrosion-resistant characteristics than the individual. Afshar et al. [9], carried out the research work on the corrosion resistance evaluation of various primers and coatings. While comparing the corrosion-resistant behaviour of different coatings, it was observed that the zinc-rich epoxy primer coating exhibited superior performance over the other types. Indirakumar and Manjunath [10], developed an anticorrosive coating using waste batteries. With the help of the intermediate layer of the battery containing manganese dioxide, the coating was prepared and applied over the rebar. While placing the coated rebar in the salt container for 30 days, it was observed that the coating attributed to lesser weight loss than the uncoated rebar. Similarly, Rajendran [11] conducted an experimental investigation to protect the meshing reinforcement of ferrocement panels from corrosion by incorporating nano-modified fly ash-based geopolymer mortar. The use of nano-geopolymer mortar on the ferrocement meshes offers 3 times improved corrosion resistant behaviour and it was suggested mainly for marine applications. Rooby et al. [12], studied the performance of a new nano-phase modified fly ash-based cement polymer covering on steel reinforcements in a corrosive environment. Five different types of coating were prepared and from the electrochemical studies and the impressed voltage test, it was concluded that the corrosion rate of nano-modified coated rebars was 76–89% lower than uncoated rebars.

From the previous research works, it was inferred that the anticorrosive coating developed so far, fails to satisfy the economic considerations. Also, the most commonly used zinc coatings are prone to the hydration process and lead to the cracking effect. Hence, a cost-effective anticorrosive coating is required to be developed. In the previous research work carried out by Rajendran and Giftlin [13], the epoxy content in the printed circuit boards was used for the synthesis of anticorrosive coatings. Based on the results, it was reported that the proportional variation of the PCB powder and the paint has different effects and the optimum 1 : 3 ratio was adopted by trial and error method. Also, while considering the research work done by Wan et al. [14], it was clear that the printed circuit board exhibited excellent corrosion resistant characteristics in aqueous sodium chloride solution with 99.6% inhibition efficiency.

Based on these conclusions, in this work, the waste-printed circuit boards were used to produce an anticorrosive coating. The nontarget materials in PCB were removed by certain pretreatments and the size of the particles was much reduced by grinding and ball milling. These nano PCB powders are mixed with the toluene by electromagnetic stirrer and they were added to paints as additives in the ratio of 1 : 3. The corrosion-resistant behaviour of the nano PCB-coated rebars were assessed by means of polarization technique, electrochemical impedance spectroscopic (EIS) technique and the results were compared with the uncoated and zinc coated specimens. To extend the applicability of the developed nano PCB-coating in the reinforced concrete construction, the nano PCB-coated rebars were embedded in the concrete cylinder as reinforcement and the corrosion-resistant behaviour of the specimen was also studied. The impressed current technique is used to accelerate the corrosion process and the amount of corrosion that took place was calculated by means of weight loss and change in diameter. To fasten up the corrosion process and to study the effect of varying the electrolyte concentration, a corrosive medium was changed by 3.5% and 10% sodium chloride solution. Also, the rate of corrosion that occurred, the deterioration time and the total cost were estimated and compared with the noncoated and zinc-coated rebars embedded in cylindrical concrete specimens. The effect of corrosion and the coating on the mechanical strength of the rebar specimen was studied by assessing the stress-strain behaviour and modulus of elasticity. In addition to this, the pull-out test was carried out to check the bond strength between the concrete and the coated rebar from which a novel, efficient, cost-effective, and sustainable anticorrosive coating was developed for both steel and concrete structures.

2. Materials and Methods

2.1. Materials and Pretreatment Method. For developing a cost-effective anticorrosive coating, initially, the waste PCB was collected, and pretreatment processes such as desoldering and immersion in hydrochloric acid were carried out to separate the target and nontarget materials. To form an anticorrosive nano PCB solution, toluene was procured from Alpha Scientific Company; Madurai was used as a dispersion agent. To assess the efficiency against corrosion, steel rebar was coated with the developed nano PCB-coating. For this purpose, steel rebars of 8 mm diameter were cut to the size of 15 cm.

2.1.1. Desoldering. On the collected waste PCB, target and nontarget materials were presented. The target material contains resistors, transistors, and the insulating layer. The plain PCB was classified as nontarget materials. In order to remove the target materials present over the PCB, the soldering technique was used, as shown in Figure 1(a). In the soldering technique, the PCB was subjected to a thermal application under the temperature of 200°C.

(a) (b) (c)

Figure 1: Pre-treatment of PCB board and production of nano PCB particles: (a) desoldering, (b) planetary monomill, and (c) FESEM image of the produced nano PCB.

2.1.2. Immersion in Hydrochloric Acid. After the completion of the soldering process, the PCB was immersed in 1 M dilute hydrochloric acid [15] for about two days for the complete removal of the insulating layer present in the waste PCB. The board was placed in an oven at a temperature of 100°C, to remove the moisture content. The chemical transition temperature of PCB starts from 130°C [16]. Due to this effect, the heating of PCB at 100°C will only involve in the removal of moisture content without significant change in the mineral phases. The immersion in hydrochloric acid only removed the insulating layer, not involved in any other chemical reaction to form new elements [17], as confirmed by the EDAX results. Also, the results of Table 1 indicates that there is no sign of existence of the target materials in the pretreated PCB powder and confirmed the complete removal of target materials from the PCB.

2.1.3. Pulverization. The treated PCB boards were broken into smaller pieces, and then they were subjected to a pulverization process. Broken pieces of the PCB were crushed manually with the help of a tamping rod for about 3 hours. After the manual crushing, the crushed particles were ground in the mixer. The size of the particle obtained from the mixer was 4.36 mm. The weight of the powder obtained by crushing 10 PCB boards was 200 g.

2.1.4. Synthesization of Nano PCB Powder. In order to attain a desirable particle size for the preparation of coating, the obtained PCB powder was grinded with the help of a Pulverisette 7, Fritsch planetary mono mill, as shown in Figure 1(b). Initially, 20 g of PCB powder sample was taken and 50 numbers of tungsten carbide balls were used for each trial. The ball to powder ratio was maintained to 1 : 17.5. Toluene was used as a coolant for the milling process. For each trial, the milling was done for 2 hours at 300 rpm. The grinding process was continuous with 7 minutes interval at every 15 minutes of milling process. After 2 hours of grinding, the PCB powder-toluene mixture was taken out from the ball mill and allowed to spread over the metal tray. The evaporation of toluene was taken place in the atmosphere temperature and the grounded nano PCB powder was separately collected by using steel spatula.

After the completion of 7 successful trials, 120 g of fine PCB powder was obtained. The size of the obtained nano PCB powder varied from 37.16 to 76.20 nm, as shown in Figure 1(c). Also, the chemical composition of the obtained nano PCB powder was studied by using EDAX analysis and the results are shown in Table 1.

2.2. Specimen Preparation

2.2.1. Coating of Rebar. The obtained nano PCB powder was mixed with toluene which acted as solvent. For this purpose, 30 g of nano PCB powder was added to the 10 ml of toluene in a conical flask. The solution was sonicated for 15 minutes to ensure thorough mixing. Based on the conclusions drawn from previous research work [13], the prepared nano PCB powder solution was mixed with paint in a ratio of 1 : 3 by volume. As the nano PCB was presonicated in liquid solvent, the dispersion of solution in the paint is easier as confirmed by Ribeiro et al. [18]. The developed nano PCB-based anticorrosive coating was applied manually over the steel rebar of 8 mm diameter, as shown in Figure 2. The coated rebar was allowed to dry for 24 hours in the free atmosphere. To compare the behaviour of the nano PCB coating, the rebars were coated with the commercially available zinc coating by using the same method.

2.2.2. Extensive Application in the Reinforced Concrete Environment. In addition to the corrosion-resistant behaviour, the efficiency of the nano PCB powder coating was assessed in the reinforced concrete applications. For this purpose, the coated rebars were embedded in the concrete cylinder to assess the corrosion resistance and bonding nature. The cylindrical concrete specimen of diameter 15 cm and height of 30 cm was cast in the grade of M30 by confirming the standards of IS 10262, as shown in Table 2. Ordinary Portland cement of grade 53 was used as a binder, manufactured sand confirming to zone II was employed as fine aggregate, and angular stones were used as coarse aggregate. The water-cement ratio was maintained at 0.45.

While casting the specimen, the rebar was kept at the centre of the specimen. After casting, the specimen was

Table 1: Chemical composition of nano PCB.

Specimen	Element composition (weight %)					
	Copper	Chromium	Vanadium	Cobalt	Nickel	Aluminium
Nano PCB powder	34.94	28.79	14.28	18.88	8.29	0.04

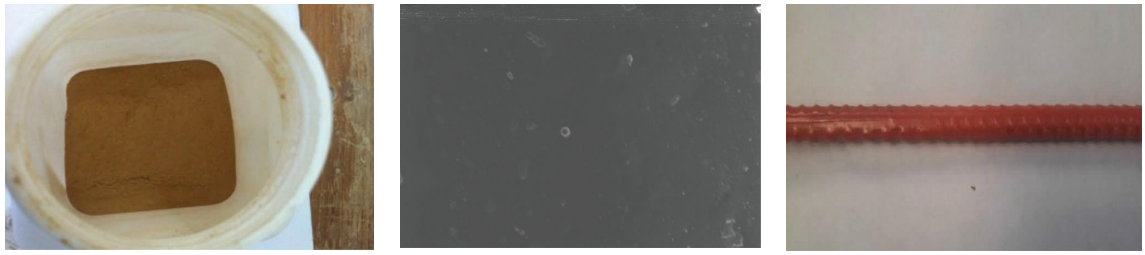

(a) (b) (c)

Figure 2: Coating of rebars with nano PCB particles: (a) nano PCB, (b) mixing of nano PCB with toluene, and (c) coating on the steel rebar.

Table 2: Mix composition.

S.no	Description	Cement (kg)	Fine aggregate (kg)	Coarse aggregate (kg)	Water
1	Ratio	1	1.66	2.63	0.45
2	Per m^3	385	639.1	1012.55	173.25

subjected to water curing for 28 days. The specimen was taken out from the curing tank and allowed to dry for 24 hours before testing.

2.3. Testing

2.3.1. Electrochemical Analysis. To assess the corrosion resistance potential of the uncoated, zinc-coated, and nano PCB-coated steel rebar, electrochemical impedance spectroscopy (EIS) and polarization techniques were employed. The uncoated and coated rebar electrodes were placed in a 3.5% sodium chloride solution. In addition to this, steel rebar coated with commercially available anticorrosive paint was also taken for EIS analysis in order to compare the corrosion-resistant behaviour of the developed nano PCB coating with the existing practice. Small sinusoidal amplitude and the voltage of 5–50 mV were applied to the specimen over the frequency range of 0.001 to 10^5 Hz. The specimen was immersed in the sodium chloride electrolyte solution, as shown in Figure 3. While applying the current on the specimen, an electromotive force is induced on the specimen and produced a corrosive environment. From the results, the phase angle difference between the input voltage and the output current was noted and plotted using the TAPEL graph.

2.3.2. Impressed Current Technique. Generally, corrosion is a long process and it takes more time. In order to increase the rate of corrosion, the impressed current technique was used. Here the corrosion was induced by applying an electrochemical potential between the reinforced bar (anode) and stainless steel plate (cathode), and 3.5% and 10% sodium chloride solutions were used as electrolytes in order to study the variation based on the speed of the corrosion process, as shown in Figure 4. This technique was used to increase the rate of corrosion for both coated and uncoated rebar. Also, the same procedure was used to assess the corrosion-resistant behaviour of the nano PCB-coated rebar surrounded by the concrete medium. The test was carried out for three different voltages of 2 V, 4 V, and 6 V. The amount of corrosion that takes place was measured by weight loss and change in diameter by visual observations.

2.3.3. Tension Test. The mechanical strength of the steel rebar in the cylindrical concrete specimens before and after different levels of corrosion was studied by conducting a tension test by confirming the standards of ASTMA615. The noncoated, zinc, and nano PCB-coated steel rebars subjected to accelerated corrosion under 2 V, 4 V, and 6 V electrode potential for 48 hours were placed in the Universal Testing Machine (UTM). A uniaxial tension was applied constantly in the steel rebars until the specimen broke. The corresponding stress corresponding to different strain levels was directly read by the data analogue system connected with the specimen. The point at which a sudden drop occurs at the stress-strain plot (i.e.) the change in elasticity is known as yield stress, and the point at which the specimen undergoes maximum stress is known as ultimate stress. By comparing the results, the change in the tensile strength of the specimen before and after corrosion was studied for noncoated, zinc-coated, and nano PCB-coated rebars.

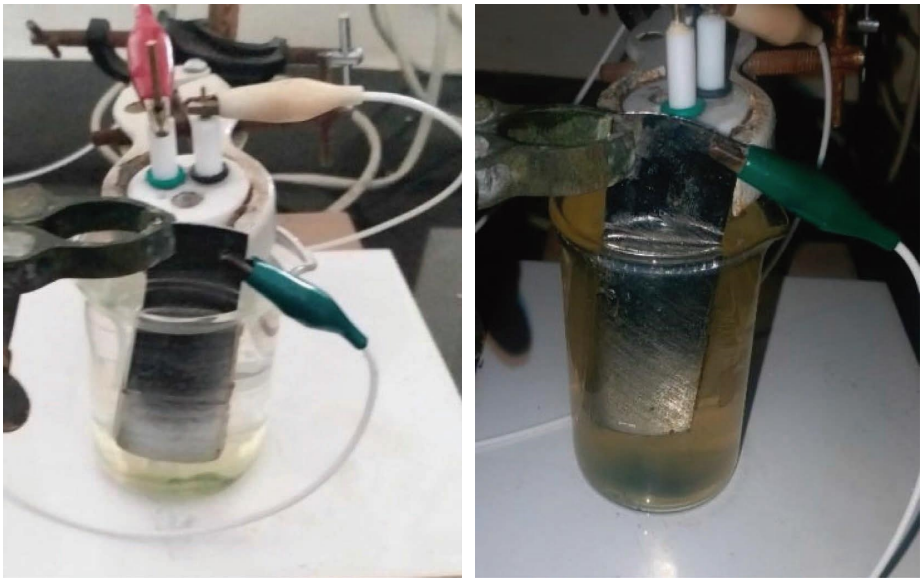

Figure 3: Electrochemical impedance spectroscopy.

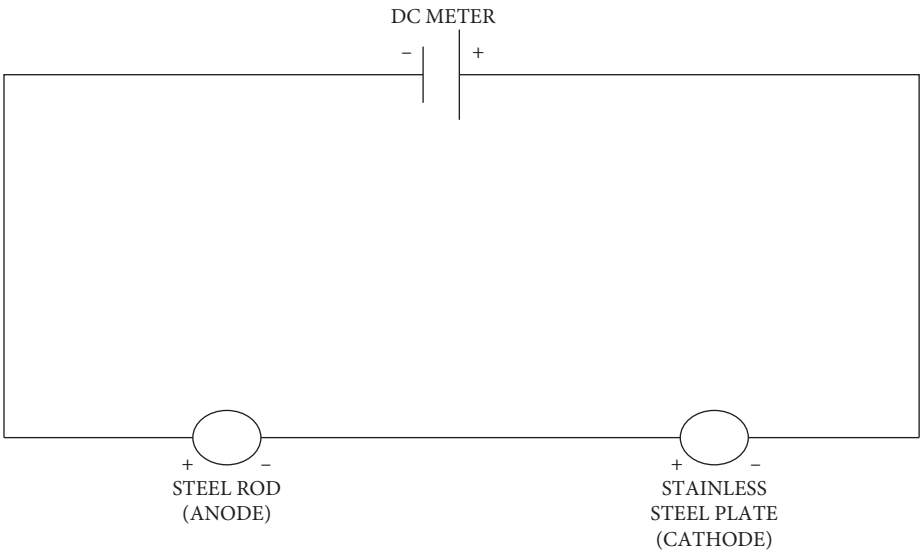

(a)

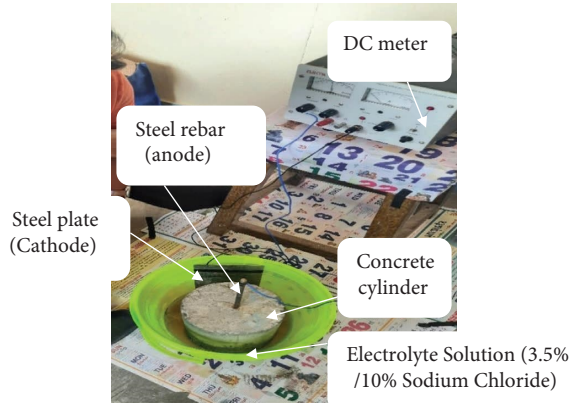

(b)

Figure 4: Accelerated corrosion test. (a) Schematic representation of electrical layout and (b) test arrangements.

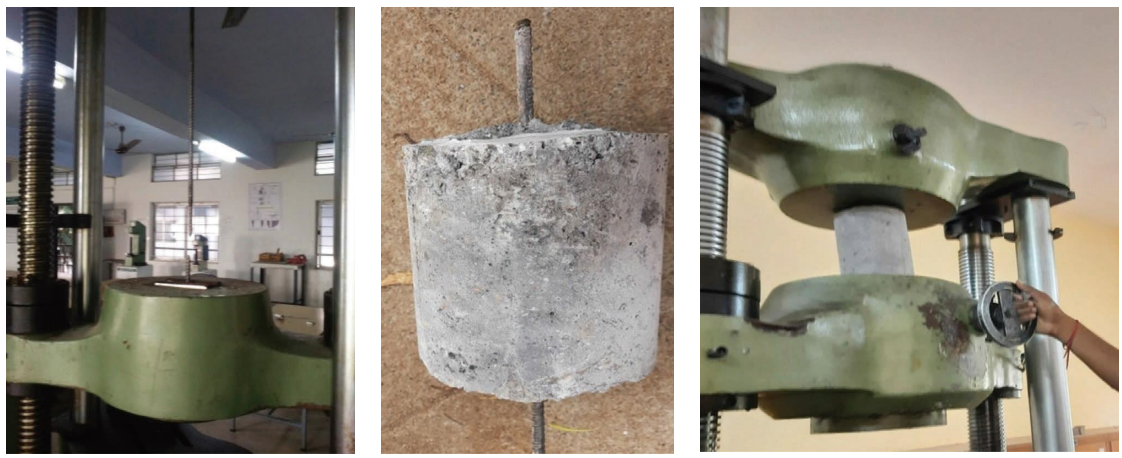

(a) (b) (c)

Figure 5: Testing of specimens: (a) tensile strength test of rebar, (b) specimen preparation for pull-out strength test, and (c) pull-out strength test.

2.3.4. Pull-Out Test. To ensure the bond behaviour between concrete and nano PCB-coated rebar, the pull-out test was carried out by confirming the standards of IS 2770-Part 1 (2017). The cylindrical specimen of height 300 mm and a diameter of 150 mm were cast. After 28 days of water curing, the cylindrical concrete specimen with uncoated, zinc-coated, and nano PCB-coated steel rebars was taken out and allowed to dry for 24 hours at room temperature. Then the specimen was prepared for the pull-out test in such a way that the steel bar was projected on both sides of the cylinder at equal lengths of 100 mm each, as indicated in Figure 5. From the test, the load at which the steel bar was delaminated from the concrete specimen was noted as a bonding failure load.

2.3.5. Adhesion Test. The adhesion of the nano PCB-coating on the steel rebar was assessed by conducting adhesion test commonly known as a pull-off test as per the standards of ASTM D 4541. The steel probe was bonded to the surface by laser glue. After 24 hours, the probe is attached to the device and the force required to remove the probe is taken as adhesive force.

3. Results and Discussion

3.1. Electrochemical Test Results

3.1.1. Electrochemical Impedance Spectroscopy (EIS). To analyze the electrode charge transfer resistance of the coated and uncoated rebars, EIS was employed. Due to the process of induced corrosion on the rebar, the out-of-phase of the output current was noticed from the input voltage [13], which is known as impedance. The phase angle graph plotted between the input voltage and the output current is known as the Tafel plot, as shown in Figure 6. The dip in the electromotive force of the Tafel plot indicated the action of the corrosion process. In the case of uncoated rebars, the dip of the plot is observed at the input voltage of −3.75 V and yielded the output current of −0.65 log (I/A). Whereas, in the case of zinc-coated and nano PCB-coated rebars, the occurrence of a Tafel plot dip was shifted to the input voltage of −4.5 V and −6 V, respectively. This implicated that the protective character of the passive film offered by the zinc and nano PCB-coating induced the drastic shift in the corrosion dip. Also, the increase in the phase angle of the nano PCB-coated rebars indicated the improvement in the corrosion resistance. The shift in the occurrence of the corrosion dip in the Tafel plot indicates the delay in the corrosion process of the zinc-coated and nano PCB-coated rebars.

3.1.2. Potentiodynamic Polarization. The results of the dynamic polarization technique are shown in Table 3. It was observed that the corrosion coefficient CORR I (A) and rate of corrosion (g/h) were extremely high in the case of the rebar without coating. It represented that the surface of the rebar is highly susceptible to deterioration by corrosive fluids. This could be well explained from the variation of corrosion current density results. The corrosion current density initially fluctuated and increased rapidly at the beginning of the polarization test. This is due to the fact that the absences of passive film around the uncoated rebar [19]. The ionic dissolution process from the rebar on the brine solution got saturated and resulted in the stabilization of corrosion current density.

These corrosive fluids are involved in the conversion process of the ferrous compound into ferric oxides commonly known as rust during the time at which the steel rebar is in contact with brine solution. The pre-existing surface hole available for the electrolyte percolation attributed to the permeation of these corrosive fluids and fastened up the oxidation process. In the case of rebar coated with zinc and nano PCB powder, these corrosive pores were filled and the rebar surface was fully covered with heterogeneous zinc and copper atoms present in the nano PCB. This acted as a protective medium to resist the percolation of sodium

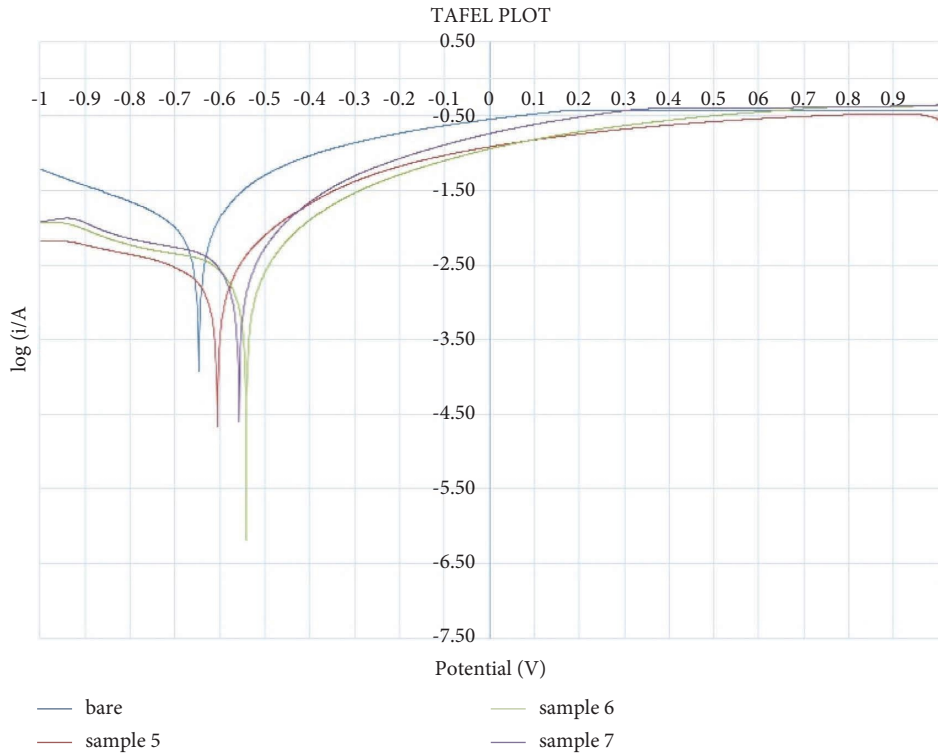

Figure 6: TAFEL plot of the specimens (bare ⟶ uncoated specimen; sample 5 ⟶ with commercial anticorrosive paint; sample 6 ⟶ zinc coated specimen; sample 7 ⟶ nano PCB-coated specimens).

Table 3: Comparison of potentiodynamic polarization test.

S.no	Description	Uncoated rebar	Zinc coated	Nano PCB coated
1	CAT slope (I/V)	3.600	5.676	5.927
2	ANO slope (I/V)	9.315	4.656	4.565
3	CAT int ($\log i$)	−3.325	−3.671	−3.693
4	ANO int ($\log i$)	−2.870	−3.545	−3.613
5	Lin Pol R (ohm)	37	159	153
6	CORR I (A)	$9.136e-0.004$	$2.398e-0.002$	$2.586e-0.002$
7	Rate (mm/year)	$4.169e+0.002$	$1.342e+0.002$	$1.319e+0.002$
8	Rate (Angs/min)	$2.014e+0.002$	$5.780e+0.01$	$5.931e+0.01$
9	Rate (gram/h)	$9.518e-0.004$	$3.012e-0.002$	$2.96e-0.002$

chloride corrosive fluid and the oxidation of the rebar surface. Also, the finer nanograins and smoother surface of the nano PCB powder exhibited lowest corrosion density. Due to this effect, the rebar coated with zinc and nano PCB powder resulted in a 3 and 3.5 times reduced rate of corrosion when compared to the uncoated rebars. Also, it is inferred that the derived nano PCB coating exhibited an almost similar protective corrosion resistant mechanism as that of the existing zinc coating and confirms the application of a protective anticorrosive coating.

3.2. Physiochemical Results

3.2.1. Degree of Corrosion. From the results of the accelerated corrosion test, it was observed that the degree of corrosion increased with the increase in immersion time and the maintained potential difference. This indicates the deterioration rate of the specimen in terms of weight and is calculated by using the following equation:

$$\text{Degree of corrosion} = \frac{(W\text{o} - W1)}{W\text{o} * 100}. \quad (1)$$

Wo is the initial weight of the specimen before corrosion. $W1$ is the deteriorated weight of the specimen after corrosion. The increase in the degree of corrosion for the noncoated, zinc coated, and nano PCB-coated specimens were compared with respect to time, as shown in Figure 7.

The maximum degree of corrosion observed in the noncoated steel rebars was 20%, 55%, and 82% at the end of 48 hours while inducing the potential difference of 2 V, 4 V, and 6 V, respectively, when the concentration of electrolyte solution is 10% of sodium chloride solution. When the uncoated specimen was immersed in a 3.5% sodium chloride

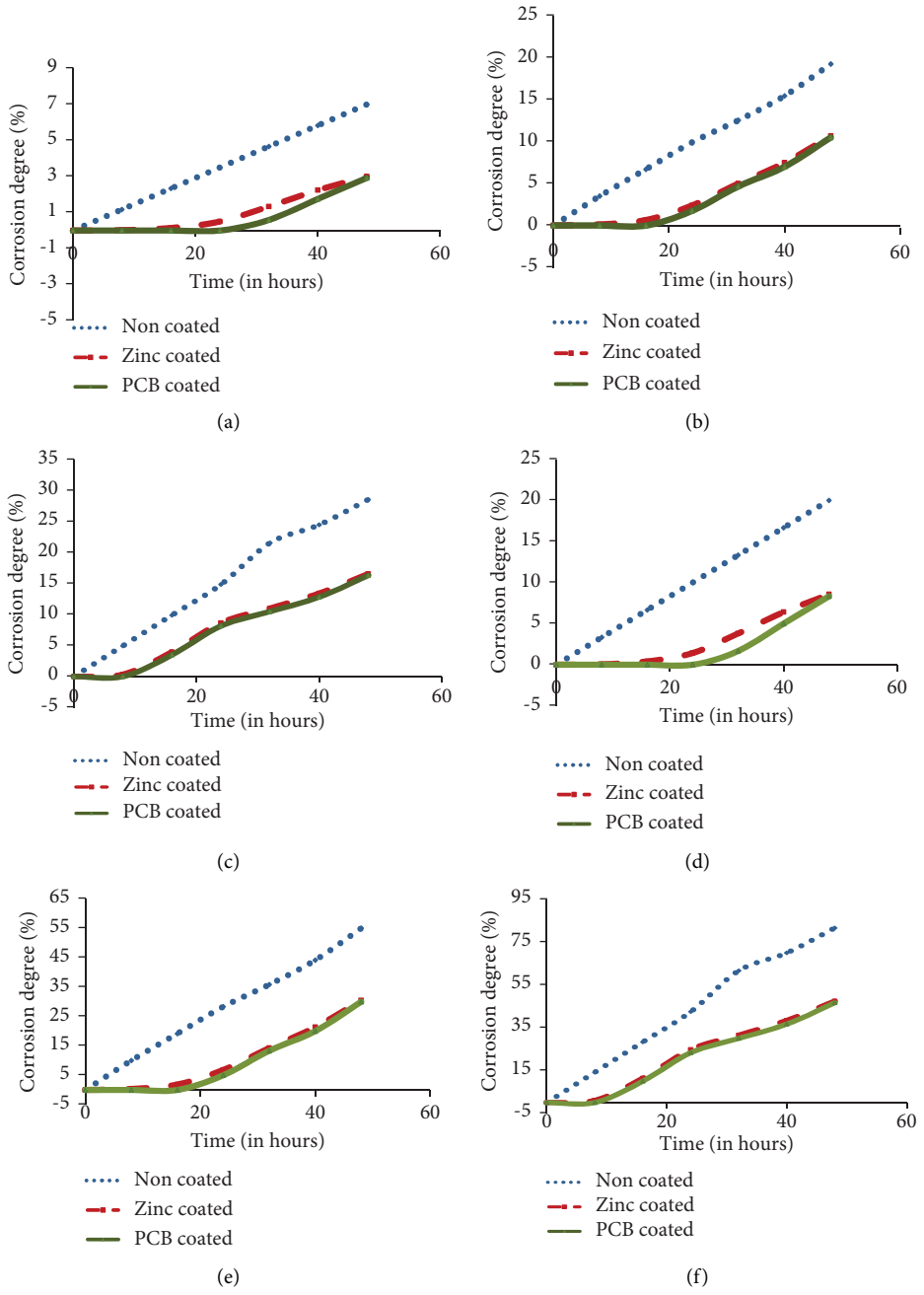

Figure 7: Comparison of degree of corrosion. (a) 2 V (3.5% NaCl), (b) 4 V (3.5% NaCl), (c) 6 V (3.5% NaCl), (d) 2 V (10% NaCl), (e) 4 V (10% NaCl), and (f) 6 V (10% NaCl).

solution, the degree of corrosion got varied by 7%, 20%, and 27%, respectively, under 2 V, 4 V, and 6 V potential differences. The rate of corrosion varied significantly with respect to the concentration of electrolyte solution. The increase in the degree of corrosion resulted in the extension of the depth and number of corrosion pits on the steel surface. The extended pits joined each other and occurred as general corrosion. When compared to the coated specimens, the noncoated steel specimens exhibit a rapid increase in the degree of corrosion. When the steel surface was in contact with sodium chloride, the oxidation reaction was taken place and the electrons were generated. To maintain the equilibrium, the electrons were consumed by the cathode unit of metal sheets which formed the hydrogen molecules [20, 21]. These hydrogen molecules are surrounded near the surface of the steel bars and hold back the generation of electrons from the anode unit in which the state of the cathode is known as the polarized state. The presence of oxygen consumed the free electrons and broke the hydrogen layer through which the depolarization reaction was taken place. This led to the induction principal corrosion reaction, as shown in the following equation

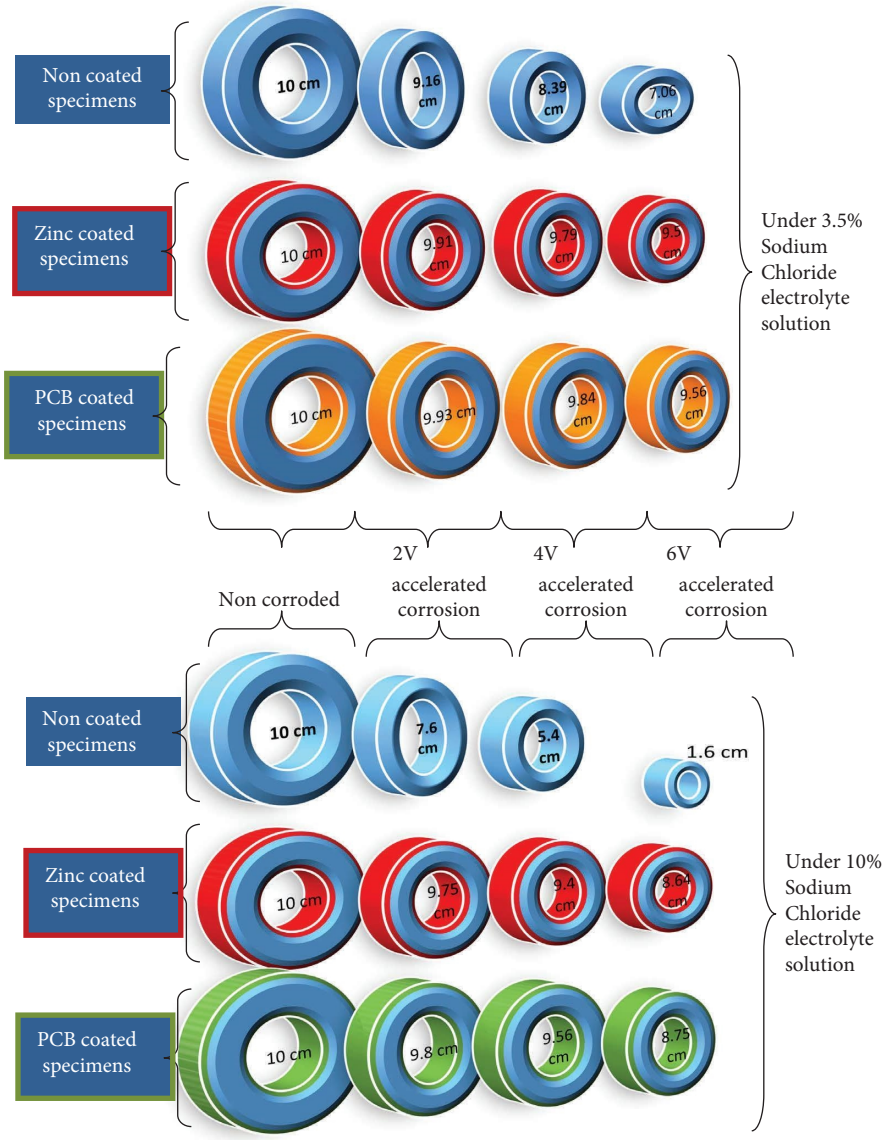

Figure 8: Comparison of change in diameter of the specimens.

$$Fe + H_2O + 0.5O_2 \longrightarrow Fe(OH)_2. \quad (2)$$

The resultant product ferrous hydroxide formed as whitish deposits around the specimen. The continuous oxidation of ferrous hydroxide formed the final product ferric hydroxide commonly known as reddish brown rust. The deposition of these rust layers indicates the rate of corrosion. As the oxidation process increased with respect to time, the corresponding formation of rust also increased further. This resulted in a more rate of deterioration in the weight of the steel bars which induced the degree of corrosion. Similarly, the higher the electric potential difference maintained between the electrodes, the greater the oxidation reaction which resulted in the rapid increment in the degree of corrosion as indicated in Figure 8. This resulted in the rapid increment in the degree of corrosion in the 4 V and 6 V conditions by 1.75–2.75 times and 3.08–4.83 times higher than the 2 V conditioned accelerated corrosion.

While coating the steel rebars using zinc powder, the maximum degree of corrosion under 10% sodium chloride conditions, at the end of 48 hours was observed to be 9%, 30%, and 47%, respectively, while inducing 2 V, 4 V, and 6 V electrode potential difference. The application of zinc coating on the steel rebars, significantly reduced the degree of corrosion by 45–52% in the noncoated specimens. This is due to the inherent ability of zinc to form corrosion by-products. When a zinc coating is presented on the outside of the steel rebar, the reactive zinc produced the zinc patina corrosive by-products [22]. This served as an efficient barrier that kept the moisture content away from the steel rebar. Also, the sacrificial anodic characteristics of the zinc coating improved the electrical contact with the steel rebar substrate

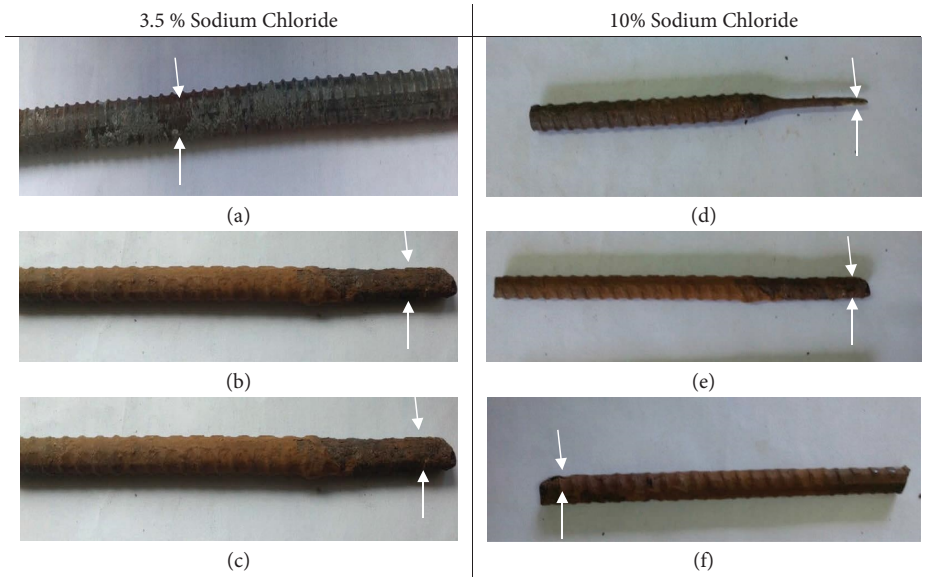

Figure 9: Corroded rebars after 6 V accelerated current. (a) Uncoated rebar (7.06 cm), (b) zinc-coated rebar (9.5 cm), (c) nano PCB-coated rebar (9.56 cm), (d) uncoated rebar (1.6 cm), (e) zinc-coated rebar (8.64 cm), and (f) nano PCB-coated rebar (8.75 cm).

and enhanced the protection against corrosion. When comparing the degree of corrosion of all the specimens, it was observed that the nano PCB-coated specimen exhibits almost similar results to Zinc-coated specimens. Due to the increase in the electrode potential from 2 to 6 V for 48 hours, the degree of corrosion in the nano PCB-coated specimens varied from 2 to 15% and 8 to 47% accordingly for 3.5% and 10% sodium chloride exposure. The degree of corrosion of the nano PCB-coated specimens was 60-45% lower than the results of noncoated specimens. The presence of chromium, vanadium, and copper ions in the nano PCB powder offered stronger covalent bonds capable enough to reduce the oxidation reaction [23]. The growth of passive resistant film around the zinc coated and nano PCB-coated rebars blocked the migration of electrolyte solution. Also, the composition of copper and chromium tends to form a self-healing oxide layer around the substrate which is attributed to the excellent resistance against the degree of corrosion.

3.2.2. Dimensional Change. The effect of corrosion induced the geometric irregularity in the section and resulted in the variation in the ribbed shape of the steel rebars. Due to the corrosion penetration, the depth of pitting varied around its circumference along the entire length of immersion. Also, the shape of the cross-section varied irregularly and resulted in a reduction in diameter, as shown in Figures 8 and 9. It was observed that the noncoated specimen experienced the highest reduction in the diameter in all the levels of accelerated corrosion. While applying the 2 V, 4 V, and 6 V electrode potential for 48 hours, the noncoated rebar of 10 cm initial diameter was reduced to 9.16 cm, 8.39 cm, and 7.06 cm under 3.5% sodium chloride and 7.6, 5.4, and 1.6 cm, respectively, at 10% sodium chloride conditions.

In the noncoated specimens, the intrusion of chloride ions exhibited superior reactivity to the hydroxide anions and reacted with the ferrous cations. The Fe^{2+} cations consumed the lone pair of electrons present in the Cl^{-} anions and resulted in the ferrous dissolution process [24]. The soluble ferrous chloride complexes diffused away from the substrate and the chloride ions migrate again in the steel rebar which induced the expansive corrosion mechanism. In each stage of corrosion, the hydroxyl ions were continuously consumed due to which the alkalinity of the specimens was largely reduced. The residual chloride ions continued to undergo a reaction with ferrous cations and the process becomes an autocatalytic mechanism [25, 26]. To compromise this auto-catalytic phenomenon of chloride-ferrous complexes, the dissolution of substrates was taken place and resulted in the corresponding rate of dimensional change in terms of diameter. This led to the highest rate of reduction in the diameter of the steel rebar. At the end of 48 hours, under 6 V potential and 10% sodium chloride conditions, the diameter of the steel rebar got highly deteriorated and only 16% of the initial diameter was present in the noncoated steel bar. The coated specimens exhibited the very little amount of geometric deterioration in all the accelerated states of corrosion. The zinc and nano PCB coating prevent oxidation by creating an electropositive protective layer [27] around the steel rebar and significantly inhibited the rate of corrosion and the corresponding reduction in the rebar diameter as compared in Figures 9 and 10. Due to this effect, the steel rebar of 10 cm initial diameter with zinc and nano PCB-coating was reduced to 9.75 cm and 9.8 cm at 2 V, 9.4 cm and 9.56 cm at 4 V, and 8.64 cm and 8.75 cm at 6 V, respectively as given in Figure 8. The reduction in the diameter due to the geometric irregularity and deterioration of various potential differences of accelerated corrosion was observed to be in the ranges of 24–84%, 2.5–13.6%, and 2–12.5%, respectively, for the noncoated, zinc-coated, and nano PCB-coated specimens. It was inferred that the efficient sealing of coating was attributed to the excellent

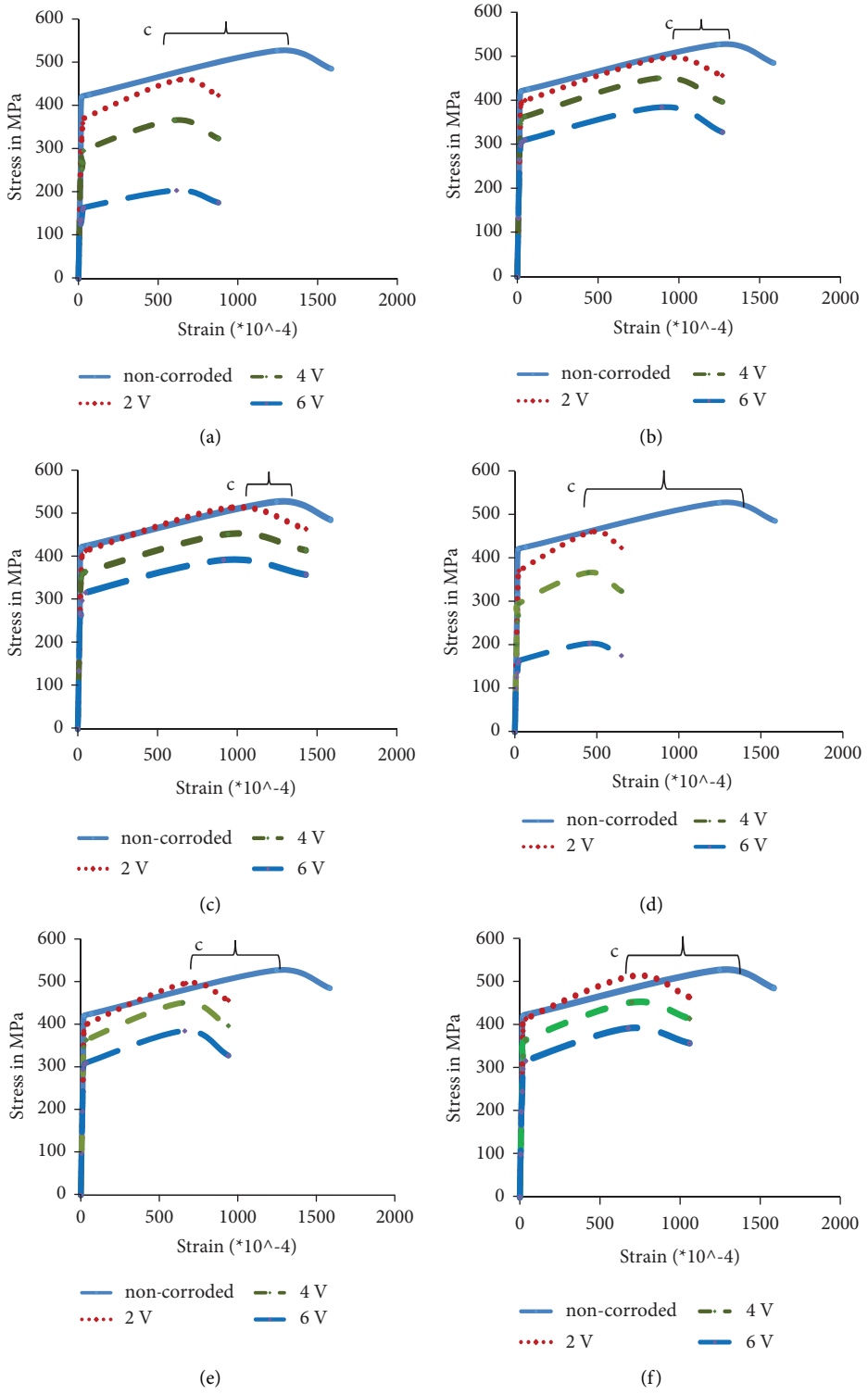

Figure 10: Comparison of stress-strain behaviour for (a, d) noncoated; (b, e) zinc coated; (c, f) nano PCB-coated rebars ("c" indicates the change in the ultimate strength). (a) Uncoated rebar (3.5% NaCl), (b) zinc coating (3.5% NaCl), (c) nano PCB-coating (3.5% NaCl), (d) uncoated rebar (10% NaCl), (e) zinc coating (10% NaCl), and (f) nano PCB (10% NaCl).

protection against corrosion and the corresponding reduction in the diameter. Also, it was observed that the nano PCB-coating exhibited similar results as that of the commercially used zinc coating and making the possibility of using the nano PCB-coating an efficient and cost-effective alternative to the zinc coating.

Table 4: Comparison of modulus of elasticity of the specimens.

S.no	Specimen	Corrosion level (percentage of sodium chloride)	Yield stress (MPa)	Ultimate stress (MPa)	Yield strain	Ultimate strain	Modulus of elasticity ($\times 10^5$) MPa
1	Noncoated	Noncorroded	426.21	528.50	0.00670	0.12462	2.160
		2 V (3.5%)	386.40	479.14	0.00260	0.04836	2.010
		2 V (10%)	371.54	460.71	0.00250	0.04650	1.930
		4 V (3.5%)	308.05	381.98	0.00250	0.04643	1.980
		4 V (10%)	296.20	367.29	0.00240	0.04464	1.901
		6 V (3.5%)	171.37	212.50	0.00255	0.04739	1.960
		6 V (10%)	164.78	204.33	0.00245	0.04557	1.882
2	Zinc coated	2 V (3.5%)	417.41	517.60	0.00374	0.06964	2.120
		2 V (10%)	401.36	497.69	0.00360	0.06696	2.035
		4 V (3.5%)	379.08	470.06	0.00364	0.06770	1.970
		4 V (10%)	364.50	451.98	0.00350	0.06510	1.891
		6 V (3.5%)	323.70	401.39	0.00370	0.06886	1.964
		6 V (10%)	311.25	385.95	0.00356	0.06622	1.885
3	Nano PCB-coated	2 V (3.5%)	431.34	534.86	0.00395	0.07351	2.130
		2 V (10%)	414.75	514.29	0.00380	0.07068	2.045
		4 V (3.5%)	380.10	471.33	0.00390	0.07254	1.970
		4 V (10%)	365.48	453.20	0.00375	0.06975	1.891
		6 V (3.5%)	329.51	408.60	0.00379	0.07041	1.960
		6 V (10%)	316.84	392.88	0.00364	0.06770	1.882

3.3. Mechanical Strength. From the results of the tension test, the stress-strain behaviour of the specimens before and after corrosion was compared as given in Figure 10. It was observed that the yield stress reduced significantly with the increase in the electrode potential and the increase in the sodium chloride concentration for all the specimens. From Table 4, it was observed that there were no significant changes in the values of modulus of elasticity and strain values for the specimens under various levels of corrosion.

It was observed that the length of the yield plateau was considerably reduced with the increase in the electrode potential irrespective of the method of coating as indicated in Figure 3. The increase in the degree of corrosion attributes to the considerable reduction in the margin of elasticity and the corresponding decrease in the length of yield plateau [22]. The increase in the degree of corrosion attributes to the increment in the intensity of yield stress.

While varying the induced corrosion level from 2 to 6 V, it was observed that the noncoated specimens exhibited an extreme reduction in the yield stress by 13–61% to the noncorroded steel rebars. The rapid deformation in the resisting cross-section of the steel rebar due to corrosion attributes to the highest rate of loss in the nominal tensile strength [23]. Also, the corrosion changed the microstructure of the steel surface and its lattice atom arrangement which makes the surface brittle and flaky. As a result, the noncoated rebar gradually loses its yield strength and elasticity, as shown in Figure 9(a). In the zinc coated and nano PCB-coated specimens, the reduction in the yield stress was observed to be 6–27% and 3–26%, respectively. The zinc coating offered a sacrificial anodic effect to the steel rebar substrate to prevent the oxidation process and the corresponding reduction in the cross-section. Also, the compositions of protective metals copper, vanadium, and chromium in the nano PCB powder exhibited higher electrochemical potential than the steel substrate to resist corrosion. These attributes to the least changes in the yield strength of steel rebar at every level of corrosion. The change in the ultimate strength of the corroded steel with uncoated, zinc coated, nano PCB-coated conditions immersed in 3.5% and 10% sodium chloride solution was indicated by the letter "c", as shown in Figure 9 and the length of parenthesis represented the shift of ultimate tensile strength from the virgin state to the most corroded state. It was inferred that the shift of the ultimate tensile strength point of the uncoated specimen under various electrode potentials was too large due to the higher amount of deterioration. This will lead to failure in the load-transferring mechanism and premature failure of the steel rebar subjected to the corrosive environment. But the shift in the ultimate point of the zinc and nano PCB-coated rebars was comparatively lower than the uncoated specimen due to the sacrificial protective coating against the induced oxidation process. This led to a significant reduction in the deterioration rate and 74% improved ultimate tensile strength of the nano PCB-coated steel rebars.

3.4. Pull-Out Strength and Adhesive Strength. From the pull-out test results, it was noticed that the specimen with noncoated rebars showed the bond strength of 7.42–7.47 N/mm^2, while the zinc and nano PCB-coated steel bars were pulled out from the concrete specimen with the bond strength value of 6.57–6.68 N/mm^2. It was inferred that the noncoated steel bars exhibited higher resistance to external pull than the coated rebars due to the strong interfacial bond. Also, from the adhesion test results it was observed that the force required to remove the uncoated, zinc coated and nano PCB-coated rebar from the concrete cylinder were 4, 3.8, and 3.7 MPa, respectively. The nano PCB-coated steel rebar exhibited similar adhesive force as that of the zinc-coated rebar which is 7% lesser than the adhesive strength of the uncoated rebar. This confirmed the results of bond strength of each rebar with the adjacent concrete specimen. The reason behind this phenomenon involved the change in the hydrophilic properties of the coated rebars. From the pilot-scale study [13], it was confirmed that the noncoated steel surface showed a water contact angle of 74° which indicates the hydrophilic nature. Whereas the nano PCB and zinc-coated specimen exhibited a contact angle of 92° and it possesses hydrophobic properties which attribute to the reduction in the bond strength (Figure 11) than the specimen with uncoated rebars [24]. But the reduction in the bond strength of nano PCB-coated specimen was only 12% of the bare specimen. Hence, the nano PCB-coated bars can be employed as corrosion-resistant steel rebars in the application of structural concrete. Also, the cost of preparation of anti-corrosive coating from nano PCB powder is comparatively lesser than the actual cost of anticorrosive paint, as shown in Table 5.

From comparing the results of existing anticorrosive paint and the zinc powder coating, the synthesized nano PCB-coating exhibited 42% and 46% lesser cost and provides a possibility of reusing the waste PCB powder economically.

3.5. Toxicity of PCB. Generally, the PCB components are the core elements of electronic wastes in which highly toxic and indisputable metals such as copper, zinc, aluminium, lead, nickel, cadmium, selenium, arsenic, barium, chromium, and mercury are presented. The PCB materials with hazardous elements are usually disposed as landfills which polluted the soil and water systems and also affect the human health and environment in various aspects. The metals of copper, zinc, and aluminium and their leaching effect resulted in the gastrointestinal distress, anaemia, digestive disturbances, and kidney dysfunction. The lead metal is the most common toxic constituent of PCBs which are present as lead to tin solders are found to leach at higher concentrations in landfills and acted as contaminants of the environment causing severe effects to the biota such as renal toxicity, hepatotoxicity, carcinogenicity, kidney dysfunction, respiratory disorders, skin allergy, selenosis, and chronic pulmonary toxicity [28]. Recycling and reusing of this toxic PCB involved on the several environmental challenges to which the developed method of nano PCB-coating will through a new light in both sustainable and economical aspects.

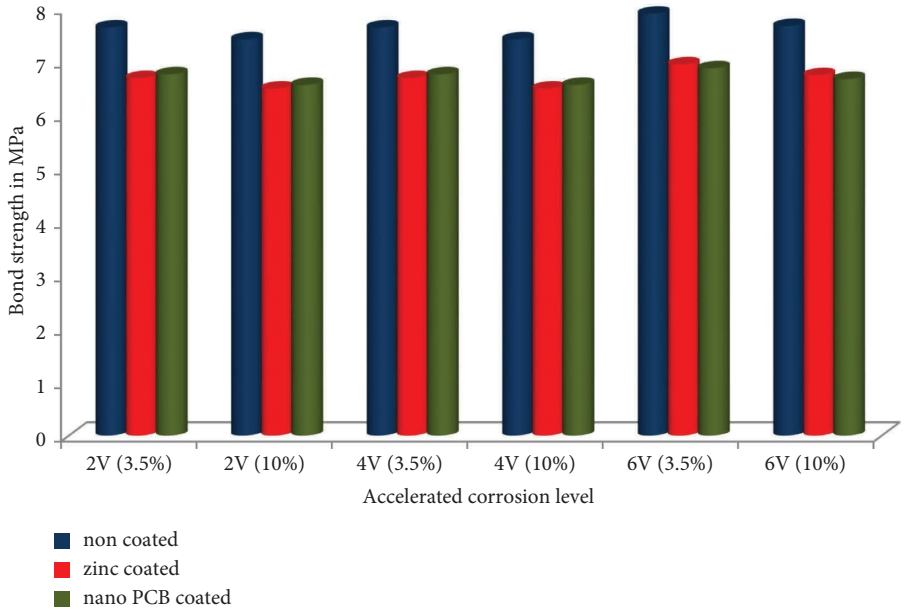

Figure 11: Comparison of bond strength.

Table 5: Cost analysis for normal anticorrosive paint with prepared zinc and nano PCB-coating.

SI. no	Description	Ingredients	Quantity (lit/ton)	Cost/lit Rs	Total cost (Rs)
1	Anticorrosive paint (commercially available in market)		9.76	350	3416
2	Zinc coating	Ordinary paint	7.32	250	1830
		Toluene	2.44	55	134
		Zinc powder	4.88 kg	350/kg	1708
			Total		3672
3	Nano PCB-coating	Ordinary paint	7.32	250	1830
		Toluene	2.44	55	134
		Nano PCB powder	4.88 kg	—	—
			Total		1964

4. Conclusion

In this paper, a novel cost-effective anticorrosive coating was derived with the help of waste nano PCB powder and the corrosion-resistant behaviour of the coating was studied with the help of impressed current techniques. The mechanical strength of the corroded rebars in the concrete specimens at various levels of electrode potential difference was studied by comparing the yield and ultimate tensile strength. The results of the nano PCB-coated steel bars were studied in both rebar and reinforced concrete applications. The bonding efficiency and adhesive strength of the nano PCB-coated steel rebars were studied by conducting a pull-out test. From the results, the following conclusions are drawn in the following:

(i) From the EIS results, it was inferred that the use of nano PCB coating exhibited a 3.5 times reduction in the rate of corrosion of steel rebars and confirms the similar resistive characteristics of existing costlier zinc coating.

(ii) The accelerated corrosion of 2–6 V under 3.5% and 10% sodium chloride conditions, induced 20–82% and 7–27% degrees of corrosion in the uncoated rebar. But, the protective nano PCB-coating provided on the steel rebar experienced only 2–15% and 8–47% degrees of corrosion while immersing in 3.5% and 10% sodium chloride exposure. The cathodic protection offered by the copper and vanadium ions in the nano PCB powder-coating induced 42.64% improved rate of resistance against accelerated corrosion.

(iii) Similarly, the deterioration caused by the corrosion effect induced 87% reduced diameter in the uncoated steel bars whereas, the nano PCB-coated steel bars exhibited only 52.5% change in dimension after applying 6 V impressed current for 48 hours.

(iv) It was observed from the EDAX results that the presence of copper, chromium, and vanadium in the nano PCB powder offered anodic protection on the embedded steel surface and showed 1.65 times

improved resistance against corrosion than the uncoated specimen.

(v) From the tension test, it was inferred that due to the creation of an electropositive layer by the nano PCB powder, the reduction in the length of yield plateau was 32% lesser than the non-coated specimens and exhibited similar performances of zinc coating.

(vi) From the pull-out test results, it was noticed that the force required to attain bonding failure between the steel and concrete was 37.71 kN and 33.18 kN, respectively, for the uncoated and nano PCB-coated specimen. Due to the hydrophobic nature of the nano PCB powder, the bonding strength was reduced slightly by 12% lower than the bare steel specimen. Further investigation on the treatment of nano PCB-coated steel bars improved the bonding efficiency.

(vii) Also, the adhesive strength of the noncoated, zinc coated and nano PCB-coated rebars varied by 4 MPa, 3.8 MPa, and 3.7 MPa, respectively. This represented that the nano PCB-coated rebars exhibited similar adhesive strength properties with 7% variation when compared to non coated rebars.

(viii) Based on the market price of the commercial anticorrosive paint it is estimated that Rs.3416 is required to provide an anticorrosive coating for a tonne of steel. By using the developed nano PCB powder as an anticorrosive coating for 1 tonne of steel, the total cost of the coating was reduced to Rs. 1964 which is 42% lesser than the commercial corrosion-resistant paint.

From the results of this work, it is concluded that the developed nano PCB-coating offered 1.65 times improved corrosion resistance to the steel reinforcement and reduced the coating cost by 42% than the commercial anticorrosive paints, and will lead to the development of structures by ensuring safety, serviceability, economy, and sustainability.

Data Availability

All data generated or analysed during this study are included in this published article.

Conflicts of Interest

The authors declare that there are no conflicts of interest.

Acknowledgments

The authors sincerely thank the management of Mepco Schlenk Engineering College, Sivakasi, for the infrastructural facilities to complete this work.

References

[1] N. Sharma, S. Sharma, S. K. Sharma, R. L. Mahajan, and R. Mehta, "Evaluation of corrosion inhibition capability of graphene modified epoxy coatings on reinforcing bars in concrete," *Construction and Building Materials*, vol. 322, Article ID 126495, 2022.

[2] C. Van Nguyen, P. Lambert, and V. N. Bui, "Effect of locally sourced pozzolan on corrosion resistance of steel in reinforced concrete beams," *International Journal of Civil Engineering*, vol. 18, no. 6, pp. 619–630, 2020.

[3] A. Al-Negheimish, R. R. Hussain, A. Alhozaimy, and D. D. N. Singh, "Corrosion performance of hot-dip galvanized zinc-aluminum coated steel rebars in comparison to the conventional pure zinc coated rebars in concrete environment," *Construction and Building Materials*, vol. 274, Article ID 121921, 2021.

[4] N. Sharma, S. Sharma, S. K. Sharma, and R. Mehta, "Evaluation of corrosion inhibition and self healing capabilities of nanoclay and tung oil microencapsulated epoxy coatings on rebars in concrete," *Construction and Building Materials*, vol. 259, Article ID 120278, 2020.

[5] N. Shaikh and S. Sheetalsahare, "Effect of impressed current on corrosion of reinforcing bar in reinforced concrete," *International Journal of Advances in Mechanical and Civil Engineering*, vol. 3, 2016.

[6] Y. C. Feng and Y. F. Cheng, "Fabrication of Halloysitenano containers and their compatibility with epoxy coating for anticorrosion performance," *Corrosion Engineering, Science and Technology*, vol. 51, pp. 489–497, 2016.

[7] M. Dixit and A. K. Gupta, "Assessment of corrosion in rebars by impressed current technique," *Lecture Notes in Civil Engineering book series*, vol. 143, 2021.

[8] R. N. Jagtap, P. P. Patil, and S. Z. Hassan, "Effect of zinc oxide in combating corrosion in zinc-rich primer," *Progress in Organic Coatings*, vol. 63, no. 4, pp. 389–394, 2008.

[9] A. Afshar, S. Jahandari, H. Rasekh, M. Shariati, A. Afshar, and A. Shokrgozar, "Corrosion resistance evaluation of rebars with various primers and coatings in concrete modified with different additives," *Construction and Building Materials*, vol. 262, Article ID 120034, 2020.

[10] G. Indirakumar and N. V. Manjunath, "Corrosion resistance coating using e-waste," *South Asian Journal of Engineering and Technology*, vol. 3, pp. 39–45, 2017.

[11] M. Rajendran, "Corrosion assessment of ferrocement element with nanogeopolymer for marine application," *Structural Concrete*, vol. 22, pp. 1–13, 2021.

[12] D. R. Rooby, T. N. Kumar, M. Harilal, S. Sofia, R. George, and J. Philip, "Enhanced corrosion protection of reinforcement steel with nanomaterial incorporated fly ash based cementitious coating," *Construction and Building Materials*, vol. 275, Article ID 122130, 2021.

[13] M. Rajendran and M. Giftlin, "Corrosion resistant coating using printed circuit board powder," *Trends in Sciences*, vol. 19, p. 6, 2022.

[14] S. Wan, Y. Cong, D. Jiang, and Z. H. Dong, "Weathering barrier enhancement of printed circuit board by fluorinated silica based superhydrophobic coating," *Colloids and Surfaces A: Physicochemical and Engineering Aspects*, vol. 538, pp. 628–638, 2018.

[15] H. Shang, S. Shao, and W. Wang, "Bond behaviour between graphene modified epoxy coated steel bars and concrete," *Journal of Building Engineering*, vol. 42, Article ID 102481, 2021.

[16] S. Shanmugam, K. Ravichandran, T. S. N. Sankara Narayanan, and M. Marappan, "Development of permanganate assisted manganese phosphate coating on mild steel," *Corrosion Engineering, Science and Technology*, vol. 49, pp. 719–726, 2014.

[17] U. Trdan and J. Grum, "Investigation of corrosion behaviour of aluminium alloy subjected to laser shock peening without a protective coating," *Advances in Materials Science and Engineering*, vol. 2015, Article ID 705306, 9 pages, 2015.

[18] D. V. Ribeiro, C. A. C. Souza, and J. C. C. Abrantes, "Use of Electrochemical Impedance Spectroscopy (EIS) to monitoring the corrosion of reinforced concrete," *Revista IBRACON de Estruturas e Materiais*, vol. 8, no. 4, pp. 529–546, 2015.

[19] Y. D. Blanco, E. C. M. Campos, C. I. R. Valdés, and J. U. Chavarín, "Effect of recycled PET (polyethylene terephthalate) on the electrochemical properties of rebar in concrete," *International Journal of Civil Engineering*, vol. 18, no. 5, pp. 487–500, 2020.

[20] M. doNascimento Silva, E. Kassab, O. GinoblePandoli, J. L. de oliveira, J. Pereira Quintela, and I. S. Bott, "Corrosion behaviour of an epoxy paint reinforced with carbon nano particles," *Corrosion Engineering, Science and Technology*, vol. 55, p. 8, 2020.

[21] Q. Zhou, C. Lu, W. Wang, S. Wei, and B. Xi, "Effect of fly ash and corrosion on bond behaviour in reinforced concrete," *Structural Concrete*, vol. 21, no. 5, pp. 1839–1852, 2020.

[22] T. Ramakrishnan, K. Raja Karthikeyan, V. Tamilselvan et al., "Study of various epoxy-based surface coating techniques for anticorrosion properties," *Advances in Materials Science and Engineering*, vol. 2022, Article ID 5285919, 8 pages, 2022.

[23] A. S Jabur, "Investigation of some parameters affecting the cathodic protection of steel pipelines," *Anti-corrosion Methods & Materials*, vol. 61, no. 4, pp. 250–254, 2014.

[24] S. H. Chu and A. K. H. Kwan, "A new method for pull out test of reinforcing bars in plain and fibre reinforced concrete," *Engineering Structures*, vol. 164, pp. 82–91, 2018.

[25] E. Diler, F. Peltier, J. Becker, and D. Thierry, "Real-time corrosion monitoring of aluminium alloys under chloride-contaminated atmospheric conditions," *Materials and Corrosion*, vol. 72, no. 8, pp. 1377–1387, 2021.

[26] C. Wu, G. Chen, J. S. Volz, R. K. Brow, and M. L. Koenigstein, "Local bond strength of vitreous enamel coated rebar to concrete," *Construction and Building Materials*, vol. 35, pp. 428–439, 2012.

[27] K. Islam, A. M. Billah, M. M. I. Chowdhury, and K. S. Ahmed, "Exploratory study on bond behaviour of plain and sand coated stainless steel rebars in concrete," *Structures*, vol. 27, pp. 2365–2378, 2020.

[28] A. Priya and S. Hait, "Toxicity characterization of metals from various waste printed circuit boards," *Process Safety and Environmental Protection*, vol. 116, pp. 74–81, 2018.